1991

Computer Vision, Descriptive Geometry, and Classical Mechanics

Christoph M. Hoffmann
Purdue University, cmh@cs.purdue.edu

Report Number:
91-073

COMPUTER VISION, DESCRIPTIVE GEOMETRY, AND CLASSICAL MECHANICS

Christoph M. Hoffmann

CSD-TR-91-073
October 1991

Computer Vision, Descriptive Geometry, and Classical Mechanics[1]

Christoph M. Hoffmann[2]

Abstract

The medial-axis transform, also called skeleton, is a shape abstraction proposed by computer vision. The concept is closely related to cyclographic maps, a tool developed by descriptive geometry to investigate distance functions, and to the solution of the eikonal equation. We discuss these connections and their implications on techniques for computing the skeleton.

1 Introduction

The medial-axis transform, also called the skeleton of a shape, was proposed in computer vision by Blum as a tool for shape recognition and abstraction [3]. Cyclographic maps were developed in classical descriptive geometry as a means to solve the problem of Apollonius, and, more generally, as a device for studying distance maps, surface curvature, and other basic geometric properties [19]. In the Hamilton-Jacobi theory, the Jacobi S function is related to both of these concepts via the eikonal equation that describes wave propagation [31]. This similarity of concepts is not surprising in view of the fact that all three notions fundamentally relate to measuring Euclidean distance, from a given geometric structure, and Blum [2] was aware of these connections. Nevertheless, how this interrelationship impacts devising algorithms for computing the skeleton, and how one might take it into account when attacking its applications seems to go unreported in the literature.

Let B be a compact set in $\mathbf{R}^2$ or $\mathbf{R}^3$, such as the boundary of a solid, that is smooth almost everywhere. Define the distance from B as follows:

$$\mathrm{dist}(p, B) = \inf\{d(p, q) \mid q \in B\}$$

[1]To appear in the proceedings of the Eurographics workshop *Computer Graphics and Mathematics*, October 1991, Genova, Italy.

[2]Supported in part by ONR Contract N00014-90-J-1599, by NSF Grant CCR 86-19817, and by NSF Grant ECD 88-19817.

where $d(p,q)$ is the usual Euclidean distance. A point q of B at distance $\mathrm{dist}(p,B)$ is called a *footpoint* of p in B. The *skeleton* with respect to B is the closure of the locus of all points not in B that have at least two distinct footpoints. Intuitively, the skeleton points have two or more geodesic paths to B. We discuss ways of conceptualizing the skeleton, and of determining it algorithmically.

From now on, we fix a domain S in $\mathbf{R}^2$ with a compact, smooth boundary ∂S. Taking $B = \partial S$, the skeleton with respect to B is just the medial axis of Blum [2], and can be defined alternatively as the closure of the locus of the centers of maximal circles inscribed in S. An inscribed circle is maximal if no other inscribed circle contains it properly. Moreover, it has been noted that the skeleton is a subset of the Voronoi diagram, [16]. If S is polygonal, then the skeleton is obtained from the Voronoi diagram by deleting the edges incident to reflex vertices.

We discuss algorithms for constructing the skeleton in 2D. Many, but not all of them generalize to the three-dimensional problem, and we will comment throughout whether and how the generalizations can be achieved. A specific difficulty is that the surfaces on which faces and edges of the three-dimensional skeleton lie are not easily described using parametric or implicit algebraics that are commonly used by the geometric modeling community. In general, the surfaces can be described exactly and practically only using the dimensionality paradigm [12], as a system of nonlinear equations.

Note that the skeleton is an informationally-complete representation of the domain S, in the sense of [24], provided we associate with each skeleton point p its distance $\mathrm{dist}(p,\partial S)$ to the boundary. It will be convenient to associate the distance as an extra coordinate, to each skeleton point. Thus, the skeleton in 2D is a three-dimensional structure, and the skeleton in 3D is a four-dimensional structure. Note that an association of the distance with every interior point defines the distance surface of Blum [2]. This distance surface also arises in cyclographic maps and in the integration of the eikonal equation.

2 Geometric Approaches to the Skeleton

The skeleton can be determined by exact or by approximate methods. The exact algorithms we discuss depend on the geometry of the set B, and so they are sensitive to the permitted shape primitives. Furthermore, extending these algorithms to the 3D problem requires careful consideration of the underlying assumptions and is by no means automatic. Often, only structural elements of the algorithms generalize. Approximate algorithms discretize the set B in various ways and are, thereafter, independent of its geometry. Roughly speaking, to generalize them reduces to devising a discretization of B in 3-space, since the subsequent processing is usually trivial to extend to higher dimensions.

2.1 The Two-Dimensional Problem

Perhaps the first efficient algorithm for constructing the skeleton of a polygonal domain is due to Preparata [22]. The underlying organization can be grasped as follows: Consider shrinking the boundary of the domain with uniform speed. In this process, some edges may become smaller and reflex vertices expand as circular arcs. At certain critical distances, however, some offset edges have reached zero length, or different parts of the shrinking boundary have come into contact. These discrete events can be found by proximity computations involving two or three elements of the original boundary. They correspond to branch points of the skeleton. Proper book keeping ensures that not all triples are subjected to this analysis. Preparata's algorithm first locates the branching points of the skeleton, and then constructs the skeleton arcs connecting them. The algorithm determines the skeleton of convex polygons in $O(n^2)$ steps.

Lee [16] gave an algorithm based on the divide and conquer paradigm that computes the Voronoi diagram of a polygonal domain. So, by deleting Voronoi edges incident to reflex vertices, the skeleton is determined. Lee's algorithm takes $O(n \log(n))$ steps. Patrikalakis and Gürsoy [21] generalized Preparata's algorithm to domains bounded by circular arcs and line segments. There is also an algorithm by Srinivasan and Nackman [28], for multiply-connected polygonal domains.

For convex polygons, the skeleton consists of line segments. Reflex vertices introduce parabolic arcs. When circular boundary elements are allowed, the skeleton may also contain segments of the other conic sections.

When the allowed boundary elements are more general, then the skeleton includes curve segments whose geometry has not been studied systematically. The customary response is therefore to approximate either the boundary or the skeleton arcs or both. Exact representations can be given but require the dimensionality paradigm — unless extensive symbolic computation is undertaken; [11].

Approximations to the skeleton have been based on Delaunay triangulation as follows: Sample the boundary of the domain, obtaining a set of points whose Delaunay triangulation respects the domain boundary. Then the centers of the circumscribed circles of the Delaunay triangles contained in the domain are approximately on the skeleton, owing to the fact that they cannot contain other points of the triangulation and so are approximately maximal inscribed circles. One can now select only those triangles whose circumcenters lie near branch points of the skeleton, [23], or make the Delaunay triangulation sufficiently dense so that all circumcenters connect to a reasonable piecewise linear approximation of the skeleton, [34]. Note that certain segments of the skeleton cannot be so approximated, as shown in Figure 1. Another method [33] approximates the domain and its interior with boxes, and classifies interior boxes by the boundary element it is provably nearest to. Boxes that cannot be so classified provide an

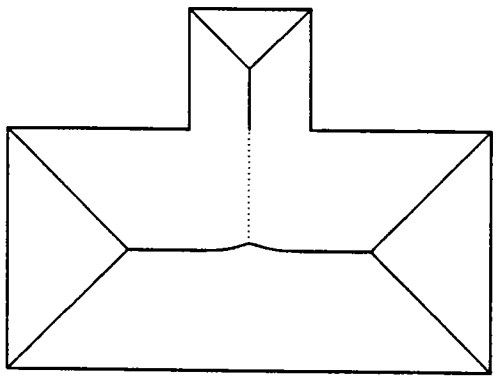

Figure 1: Dotted skeleton segment cannot be approximated through Delaunay triangulation

approximation to the Voronoi diagram.

The accuracy of the approximations can be increased using interpolation and iteration, [5]. Moreover, the approximate methods generalize to three dimensions with little change.

2.2 The Three-Dimensional Problem

The three-dimensional problem is complicated by the fact that the geometry of the skeleton surfaces is difficult; [8]. Skeleton surfaces of convex polyhedra are simple. However, nonconvex polyhedra already introduce quadric surfaces such as paraboloids and parabolic hyperboloids. More general shape primitives introduce surfaces whose geometry is not well-understood.

We are aware of only one exact algorithm; [13]. It uses many ideas of Preparata's algorithm, and, in particular, organizes the skeleton evaluation by increasing distance from the boundary. Surface construction relies heavily on the dimensionality paradigm and could well be carried out for general boundaries. However, the proximity computations make it advisable to restrict the geometry of the boundary to planes, natural quadrics, and tori. Although proximity calculations can be formulated for general geometries, the resulting systems of nonlinear equations would be difficult to solve and so the skeleton algorithm would become practically unacceptable.

The approximation algorithms all generalize, provided a suitable discretization of the surface can be given. Sapidis and Perucchio [27] describe an algorithm for constructing boundary-conforming triangulations of CSG objects. The algorithm tests whether the triangulation respects the boundary. If not, it determines which additional surface points should be added so as to eliminate tetrahedra that are partially inside and outside the solid. Such a triangulation

could be used as the basis for 3D skeleton approximation.

Several papers investigate structural properties of the 3D skeleton; [20,30]. Such studies are important when devising new skeleton algorithms, and can, in particular, guide evaluations based on marching. Yet it seems that a comprehensive topological characterization of the skeleton in 3-space is not known.

2.3 Engineering Applications of the Skeleton

Considerable work focuses on automatic mesh generation using the skeleton. It is argued that the skeleton gives good quantitative criteria for choosing the appropriate mesh density. The approaches to the two-dimensional meshing problem are especially well-developed; e.g., [1,29]. Armstrong [1] argues that quadrilateral meshes should "flow" along skeleton arcs. Srinivasan [29] gives precise criteria for subdividing polygonal regions, and grades subdomains by the relation between the length of the skeleton arc and its distance from the boundary.

Three-dimensional mesh generation using the skeleton is largely open. However, it appears that the paving approach can utilize skeleton information. This approach generates hexahedral elements layer by layer beginning at the boundary. Each layer is bounded by interior offsets of a certain depth. The skeleton indicates where the paving pattern has to be adjusted because of impending self-intersection of the layer under construction.

In unpublished work, Prinz considers feature recognition and extraction using an approximate skeleton. However, the skeleton is approximated by considering an octree subdivision [26] of the object. The skeleton approach to feature recognition has to address how the local perturbation, introduced by a feature that was added to a basic shape, affects the skeleton. If we should recognize, for example, that the global structure is rotational, will the axis of rotation still be recognizable from the skeleton after adding surface features?

Certain rigid-body transformations of the skeleton are equivalent to forming an offset of the original shape. Thus, the skeleton has potential applications in geometric tolerancing [15,14]. Stifter [30] uses the (exterior) skeleton for motion planning. By moving on the skeleton, maximum clearance from all obstacles is maintained.

3 Image Processing Algorithms for the Skeleton

Skeleton computations in computer vision begin with a digitized picture. In consequence, this problem version considers the distance of points in a regular rectangular grid from a subset of grid points that constitute the contour whose skeleton is to be found. Early algorithms by Rosenfeld [25] and Montanari [17] use a distance function that is only approximately the Euclidean distance.

Danielson's algorithm [7], in constrast, computes the Euclidean distance at each grid point with a cumulative error that is only a fraction of the grid spacing. Furthermore, if distance is expressed in multiples of the grid spacing h, the algorithm can be implemented in integer arithmetic.

Danielson's algorithm computes the Euclidean distance transform in two passes over the grid, top-to-bottom and bottom-to-top. In each pass, all rows are scanned twice, in opposite directions. The key to his method is to store at each grid point the distance *amplitudes*, i.e., the distance in the x- and y-directions to the nearest boundary grid point. While the distance from a nearest grid point is not an integer multiple of h, the distance amplitudes always are. Moreover, it is simple to compute the distance of an adjacent grid point using the distance amplitudes. Note that Danielson's algorithm generalizes trivially to 3D grids [4].

If a given set B is not discretized as a set of grid points, interpolatory schemes for computing the distance transform can be devised [5]. For example, the curve B can be approximated by a polygonal arc, where the segments are induced by the grid lines, and the adjacent grid points can be assigned the perpendicular distance to the nearest boundary segment. This improves the accuracy of the distance computation significantly, but the distance amplitudes are no longer multiples of the grid spacing. Further accuracy is obtained using iteration. For a discussion of Danielson's algorithm and such variations see [5].

Once the distance at each grid point is known, there are different methods for extracting the skeleton. Danielson suggests using the skeleton definition as the locus of the centers of maximal disks. His algorithm includes a corrective computation that compensates for errors introduced by the discretization. Other criteria are discussed in Section 6.

4 Cyclographic Maps in Descriptive Geometry

Cyclographic maps have been used in descriptive geometry to solve the Apollonius problem. The concept is due to Müller [19]. Let C be an oriented plane curve. For every point p we consider all oriented circles, also called *cycles*, that are tangent to p at C and are oriented at p in the same direction as C is. With each such cycle, we associate a point $q = (x, y, r)$, where (x, y) is the center of the cycle and r its radius. Choosing arbitrarily the counterclockwise orientation as positive, r is signed according to whether the cycle orientation is positive or negative.

When the curve point p is fixed and regular, all oriented cycles tangent at p are associated with points that lie on a line through p, with slope 1 against the (x, y)-plane and are such that the line orthographically projects onto the curve normal at p. See also Figure 2. As p varies over C, these lines comprise a ruled surface called the *cyclographic map* $\mathcal{S}(C)$ of C. Since the generators of

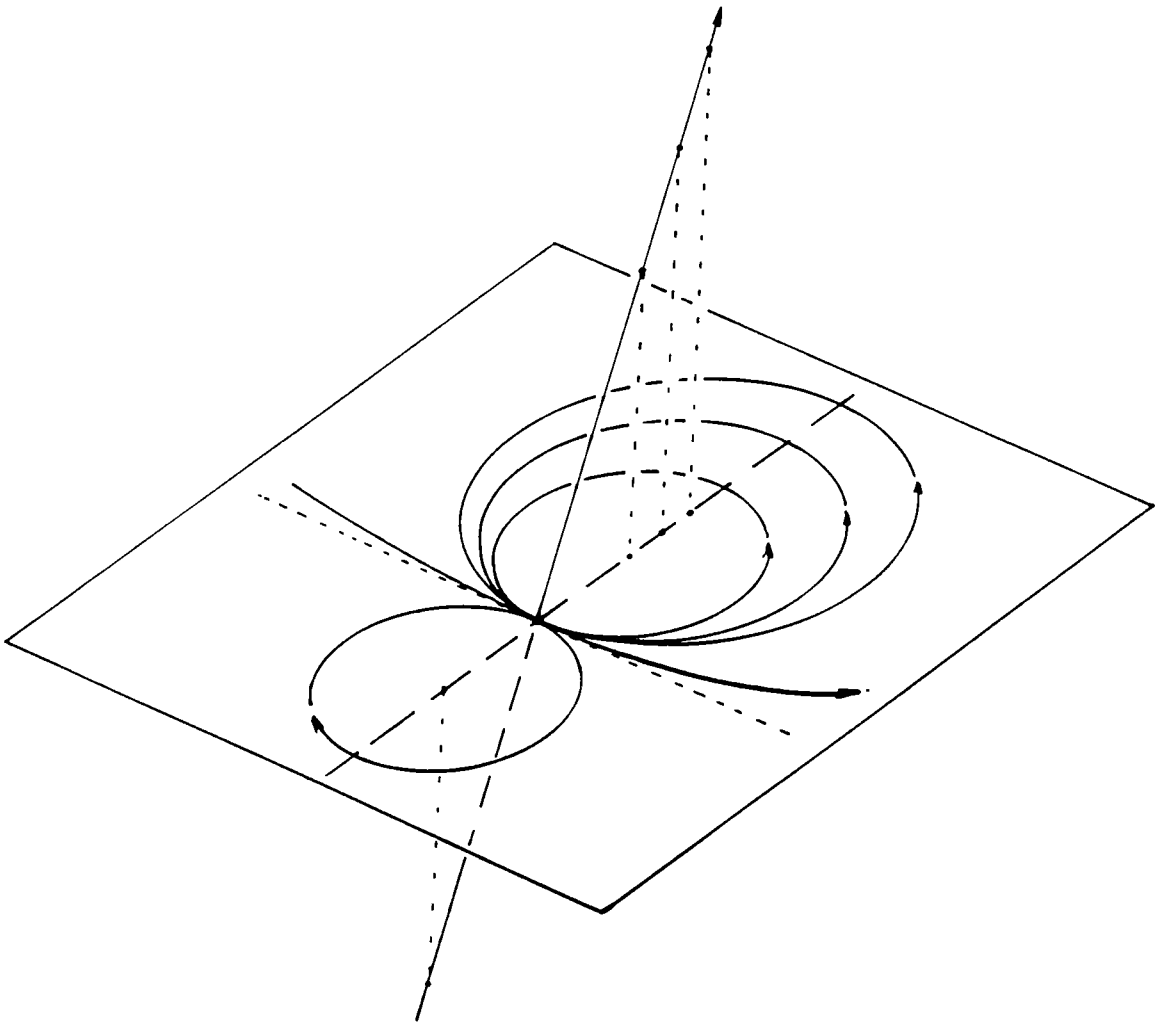

Figure 2: Cyclographic map at a curve point

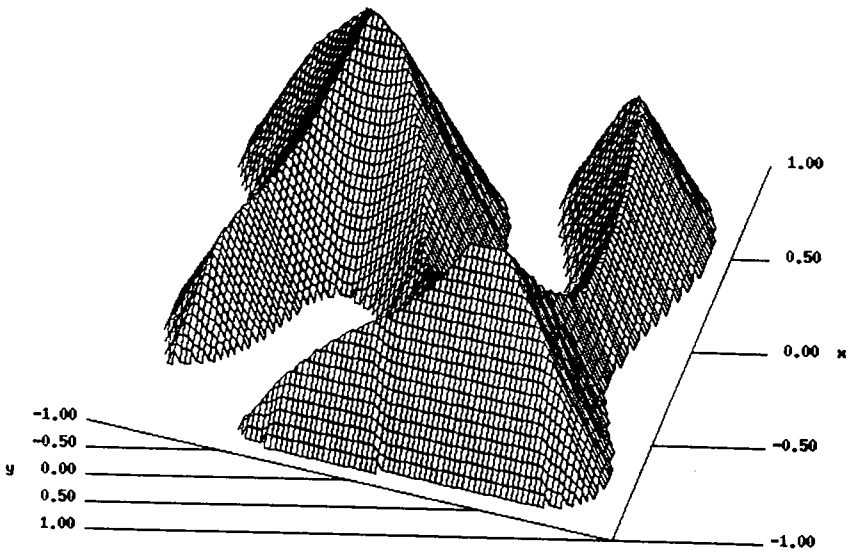

Figure 3: The surface $\overline{S}$ of a closed curve

this surface have constant slope with respect to the plane of C, the surface is developable [32].

We can restrict the surface $S(C)$ such that it is the graph of a function with the (x, y)-plane its domain. With each point (x, y) we associate the "nearest" point (x, y, r) on $S(C)$. The surface $\overline{S}(C)$ so defined is then the distance surface of Blum [2]. It follows, that $\overline{S}(C)$ can be determined approximately with the Euclidean distance transform. Figure 3 shows an example.

When intersecting the surface with a plane $r = d$ parallel to the (x, y)-plane, we obtain an offset of C by d. This is a global offset [5]. Moreover, the points on $\overline{S}(C)$ that are not continuously differentiable are the skeleton with respect to C. See also [14]. Thus, if the skeleton is known, then the map $\overline{S}(C)$ can be obtained by adding the ruling from skeleton points to corresponding footpoints on the curve. Curve points can be found directly from the skeleton point and its tangent(s), [19]. Briefly, project the skeleton point $P = (x, y, r)$ orthographically into the (x, y)-plane, obtaining a point $P' = (x, y)$. Find the intersection of the tangent to the skeleton with the (x, y)-plane, obtaining a point Q. Now draw the two tangents from Q to the circle with radius $|r|$, centered at P'. Then the contact points R_1 and R_2 are points of C. See also Figure 4.

In principle, cyclographic maps extend to three dimensions [18]. For instance, instead of oriented circles we now use oriented spheres, adding the radius as additional fourth coordinate, properly signed. The constructions and relationships mentioned before generalize to the three-dimensional case. It is also possible to replace oriented circles with suitably chosen conics. In this case the surface $S(C)$ corresponds to noneuclidean metrics.

5 Classical Mechanics and the Skeleton

Consider a continuum of particles situated at time $t = 0$ on a plane, smooth curve C, moving at constant velocity in a direction locally normal to C. By

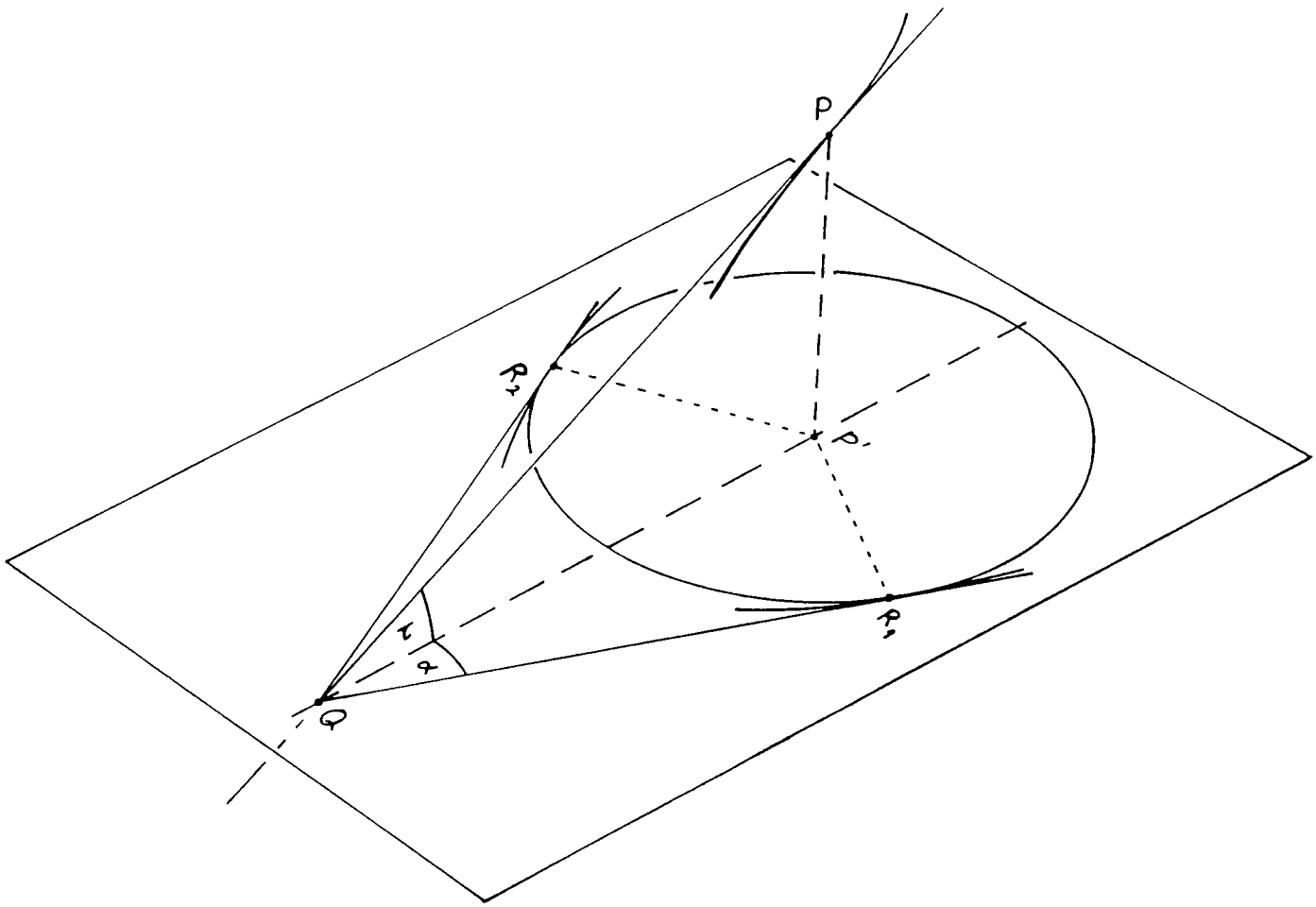

Figure 4: Recovering C from the Skeleton

the conservation of momentum, the kinetic energy of each particle is constant, and will be proportional to the squared velocity components in the principal directions. That is, $v_x^2 + v_y^2 = 1$, where v_x is the velocity in the x-direction, and v_y is the velocity in the y-direction. With $v_x = \partial S/\partial x$ and $v_y = \partial S/\partial y$, we obtain

$$\left(\frac{\partial S}{\partial x}\right)^2 + \left(\frac{\partial S}{\partial y}\right)^2 = 1$$

This is the eikonal equation in geometric optics [9], and $S(x, y)$ is the time when a particle reaches the point (x, y). Since we have assumed constant velocity, $S(x, y)$ is just the distance function assigning to each point in the plane its distance from C.

Let $p = (x, y)$ be a point reached by two or more different particles at the same time. Then p has two or more foot points on C and is therefore a skeleton point. Thus, the derivative discontinuities of the surface S are the skeleton of C. Moreover, the surface S is just the surface $\overline{S}(C)$ of the cyclographic map. We can thus think of the eikonal equation as a differential description of the Euclidean distance function; [10]. The three-dimensional form of the equation is

$$\left(\frac{\partial S}{\partial x}\right)^2 + \left(\frac{\partial S}{\partial y}\right)^2 + \left(\frac{\partial S}{\partial z}\right)^2 = 1$$

The eikonal equation suggests computing the distance function using techniques from numerical analysis. Once the distance function has been determined, the skeleton can be extracted either by applying the definition of maximal circles, as suggested in [7], or by finding the tangent discontinuities of the surface, or by processing intersecting characteristics directions during integration.

6 Computational Approaches

Once the distance map has been computed, the skeleton can be extracted by applying the maximal-disk criterion. Intuitively, we want to check whether the disk at (i, j) is contained in a disk centered elsewhere.

Given a grid point (i, j) with distance amplitudes (a, b), let $(i + r, j + s)$ be a neighbor grid point with distance amplitudes (a', b'), where $r, s \in \{-1, 0, +1\}$, with h the grid spacing. Let $d_1 = \sqrt{a^2 + b^2}$ and $d_2 = \sqrt{a'^2 + b'^2}$. If $r = 0$ or $s = 0$, and if

$$d_2 - d_1 \geq h$$

then the inscribed disk centered at $(i+r, j+s)$ of radius d_2 contains the inscribed disk centered at (i, j) of radius d_1. Therefore, the point (i, j) cannot be a skeleton point. Similarly, if $r \neq 0$ and $s \neq 0$, and if

$$d_2 - d_1 \geq h\sqrt{2},$$

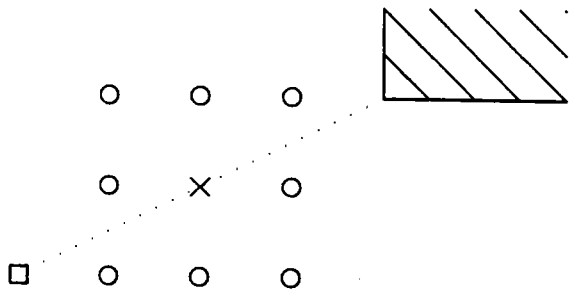

Figure 5: Disk centered at $\times$ is not maximal, yet is not contained in disk centered at the immediate neighbors

then the inscribed disk centered at $(i+r, j+s)$ of radius d_2 also contains the inscribed disk centered at (i,j) of radius d_1. Again, the point (i,j) cannot be a skeleton point in this case. If the disk at (i,j) is not contained in the disks centered at each of the eight neighbors, however, then (i,j) is not necessarily a skeleton point. In Figure 5, the disk centered at $\times$ is not contained in any disk centered at the immediate neighbors. Yet the disk is contained in a disk centered at the grid point indicated by a box.

To decide whether a disk is maximal, we instead attempt to "grow" it. Consider the situation shown in Figure 6. We try to enlarge the disk centered at $\times$ in the direction of the characteristic through the point. The extrapolated distance d_1 to the boundary along the characteristic is compared with the interpolated distance d_2 obtained from nearby grid points. If the distances agree, subject to a suitable tolerance, then the disk can be so enlarged, and the grid point $\times$ is not a skeleton point.

The computation is as follows: Let d_0 be the distance of the grid point P.

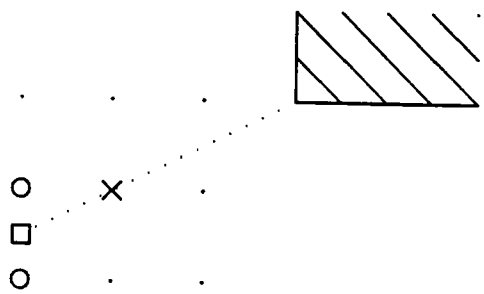

Figure 6: Disk centered at $\times$ is not maximal if it is contained in disk centered at the square.

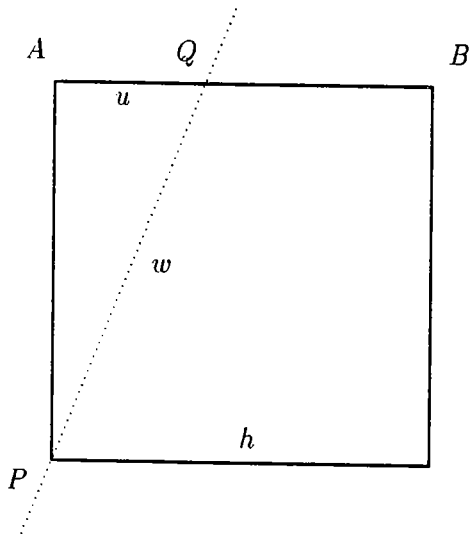

Figure 7: Extrapolating along the characteristic of P

Extrapolating from P, we obtain a point Q at distance $d_1 = d_0 + w$ from the boundary, where w is the distance $\overline{P,Q}$; see also Figure 7. Note that the slope of the characteristic is 1. The distance of Q can be determined alternatively by interpolating the distances d_a of A and d_b of B, as $d_2 = d_a + u(d_b - d_a)/h$. If the characteristic through P extends on the distance surface to Q, then the two distances will agree fairly closely. If the characteristic does not extend, however, then d_2 should be smaller than d_1 on account of Q being closer to the boundary in a different direction. Let P' and Q' be the points on the distance surface above P and Q respectively, where we assume that Q' is at height d_2. The line $\overline{P',Q'}$ has the slope $\tan(\phi) = (d_2 - d_0)/w$. If $\tan(\phi) \geq t$ for $t = 1.0$, then the characteristic through P extends, and P is not a skeleton point. But if $\tan(\phi) < t$, then the characteristic does not extend.

When we extract the skeleton from the discrete distance surface, computed by Danielson's algorithm, the discretization of the boundary has created tangent discontinuities on the distance surface that are not skeleton points. Figure 8 shows an example in which the tolerated deviation is very small, using $t = 1$. If we lower the threshold t, then less points are considered skeleton points. In Figure 9 a looser tolerance has been used, and there are fewer nonskeleton points reported. However, too large a tolerance also loses skeleton points at which the tangent discontinuity of the distance surface is relatively small.

It is simpler to account directly for the boundary geometry and use iteration to eliminate the discretization errors altogether. We now sketch a preliminary technique for extracting the skeleton assuming there is a continuous boundary

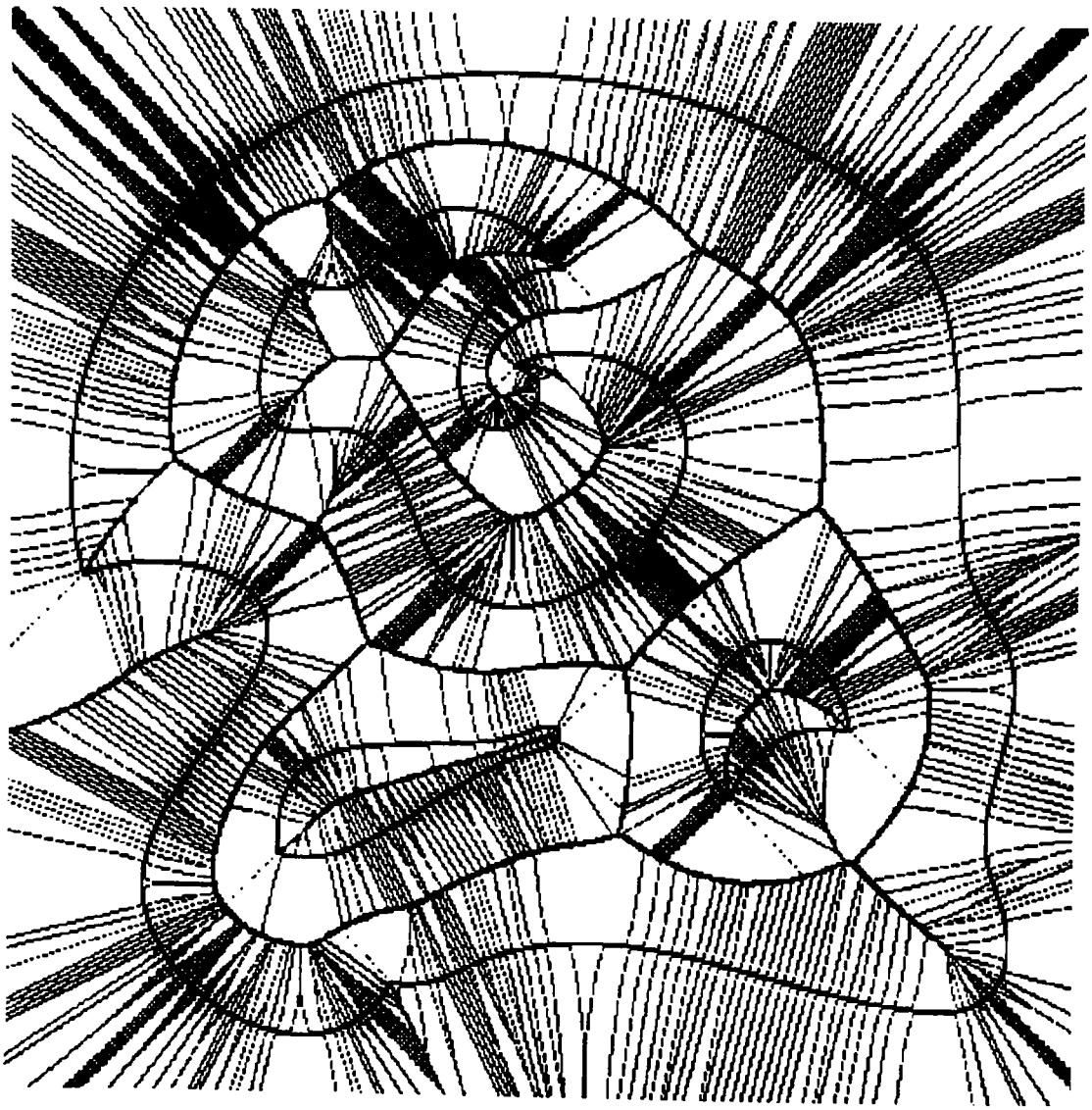

Figure 8: Discretization error affecting skeleton construction: threshold $t = 1$.

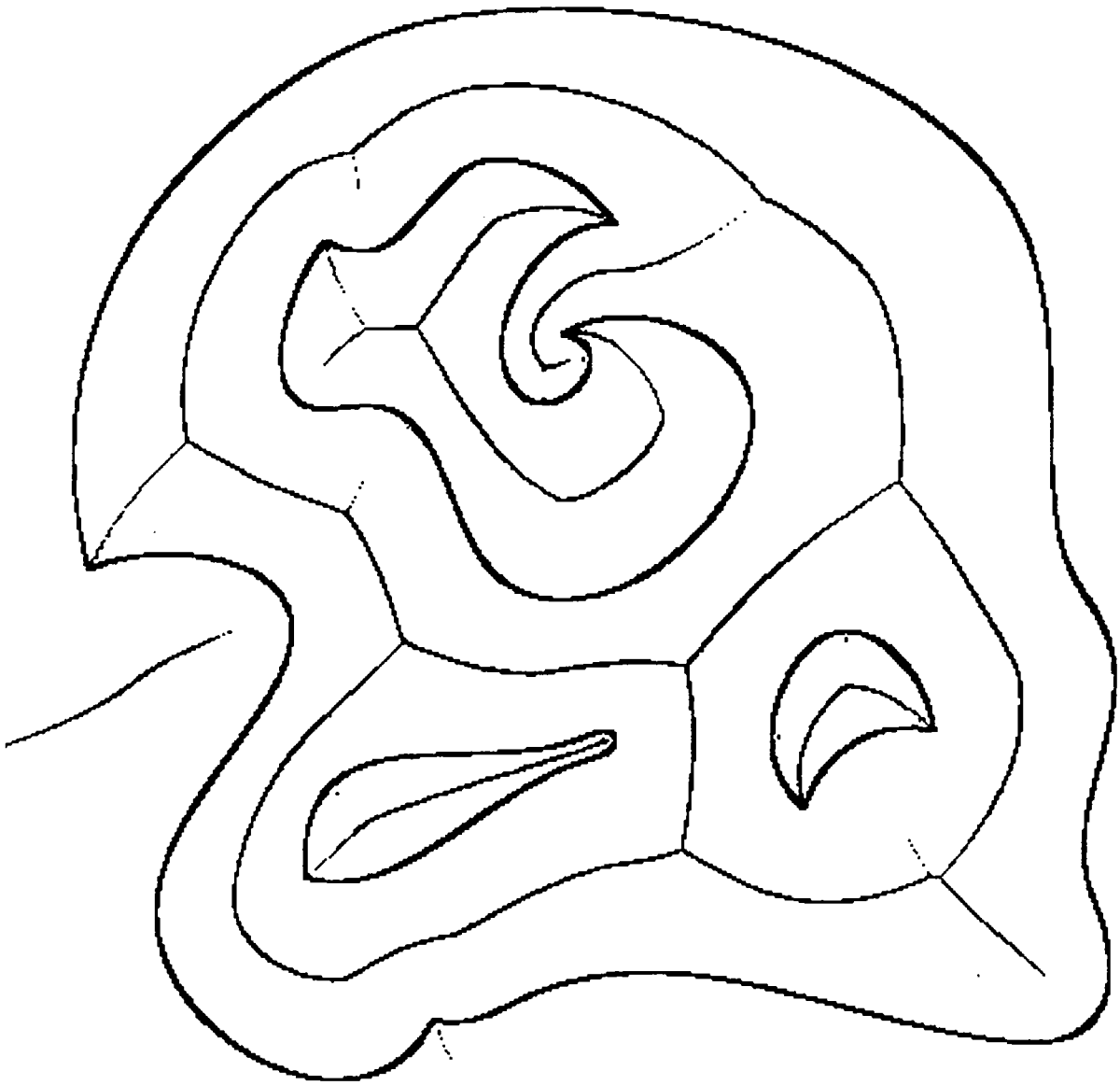

Figure 9: Effect of looser tolerance; $t = 0.6$

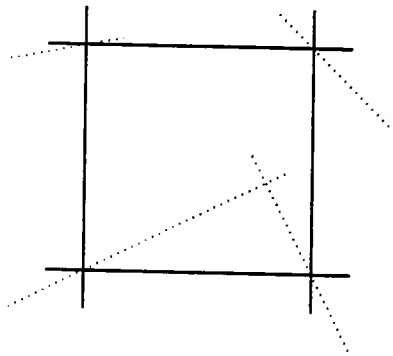

Figure 10: Approximate skeleton point at intersecting characteristics

that has been specified. The method includes iteration and interpolation steps, and applies techniques from [6,12]. First, we give a different criterion for finding skeleton points.

Consider a grid square such as the one shown in Figure 10. The characteristics of the distance function can be reconstructed from the distance amplitudes, provided that Danielson's algorithm is modified to record signed amplitudes. In the figure, the characteristics are shown as dotted lines. If the characteristics of the corner points intersect in the grid square, then the intersection point is an approximate skeleton point. This intersecting-characteristics criterion works well except near endpoints of the skeleton, because there the characteristics are nearly parallel. Note that the intersection is also difficult to determine for nearly anti-parallel characteristics. However, in that case distance interpolation will locate the intersection quite accurately.

Skeleton points lie on equal-distance curves and surfaces [8]. Since the characteristics localize which parts of the boundary lie nearby, it is not difficult to formulate a system of equations that describes the skeleton locally [13], in terms of the coordinates of the skeleton point, its footpoints, and the distance to the boundary. This system can be solved with Newton iteration very effectively since the characteristics provide good initial estimates for all quantities.

In three dimensions, matters are more complicated since the characteristics through the vertices of a grid cube will be skew in general. By interpolating the characteristics along grid edges, intersection curves and surfaces can be determined and thereafter refined using iteration in the same way as in the two-dimensional case. Alternatively, the intersections of the skeleton with grid lines can be found using interpolation.

This algorithm has not yet been fully implemented. Note that the local topological structure of the skeleton can be determined as described in [13]. In essence, our approach negotiates a reduction in the number of grid points

against the increased computational work of iteration and interpolation.

Acknowledgements

Much of the work reported here is an outflow of discussions with C.-S. Chiang, R. Lynch and H. Pottmann.

References

[1] C. Armstrong, T. Tam, D. Robinson, R. McKeag, and M. Price. Automatic generation of finite element meshes. In *SERC ACME Directorate Research Conference*, England, 1990.

[2] H. Blum. Biological shape and visual science, part I. *Journal of Theoretical Biology*, 38:205–287, 1973.

[3] H. Blum. A transformation for extracting new descriptors of shape. In W. Whaten-Dunn, editor, *Models for the Perception of Speech and Visual Form*, pages 362–380, MIT Press, Cambridge, MA, 1967.

[4] G. Borgefors. Distance transformations in arbitrary dimensions. *Comp. Vision, Graphics Image Processing*, 27:321–345, 1984.

[5] C.-S. Chiang, C. M. Hoffmann, and R. E. Lynch. *How to Compute Offsets Without Self-Intersection.* Technical Report CAPO-91-35, Purdue University, Computer Science, 1991.

[6] J.-H. Chuang. *Surface Approximations in Geometric Modeling.* PhD thesis, Purdue University, Computer Science, 1990.

[7] P.-E. Danielsson. Euclidean distance mapping. *Computer Graphics and Image Processing*, 14:227–248, 1980.

[8] D. Dutta and C. Hoffmann. A geometric investigation of the skeleton of CSG objects. In *Proc. ASME Conf. Design Automation*, Chicago, 1990.

[9] H. Goldstein. *Classical Mechanics.* Addison-Wesley, Reading, MA, 1986.

[10] A. Goodman. A partial differential equation and parallel plane curves. *American Mathematical Monthly*, 71:257–264, 1964.

[11] C. M. Hoffmann. Algebraic and numerical techniques for offsets and blends. In S. Micchelli M. Gasca, W. Dahmen, editor, *Computations of Curves and Surfaces*, pages 499–528, Kluwer Academic, 1990.

[12] C. M. Hoffmann. A dimensionality paradigm for surface interrogation. *CAGD*, 7:517–532, 1990.

[13] C. M. Hoffmann. How to construct the skeleton of CSG objects. In A. Bowyer and J. Davenport, editors, *The Mathematics of Surfaces IV*, Oxford University Press, 1990.

[14] C. M. Hoffmann and G. Vaněček. Fundamental techniques for geometric and solid modeling. In C. T. Leondes, editor, *Advances in Control and Dynamics*, Academic Press, 1991.

[15] C. M. Hoffmann and G. Vaněček. On alternate solid representations and their uses. In *Proc. DARPA Manufacturing Workshop*, Salt Lake City, Utah, 1991.

[16] D. T. Lee. Medial axis transformation of a planar shape. *IEEE Trans. Pattern Anal. and Mach. Intelligence*, PAMI-4:363–369, 1982.

[17] U. Montanari. Continuous skeletons from digitized images. *JACM*, 16:534–549, 1969.

[18] E. Müller. Zusammenhang zwischen relativer Flächentheorie und einer Verallgemeinerung der Zyklographie. *Jahresber. Dtsche. Math. Ver.*, 155–160, 1923.

[19] E. Müller and J. Krames. *Die Zyklographie.* Franz Deuticke, Leipzig und Wien, 1929.

[20] L. R. Nackman and S. M. Pizer. Three-dimensional shape description using the symmetric axis transform I. *IEEE Transactions on Pattern Analysis and Machine Intelligence*, PAMI 7:187–205, 1985.

[21] N. Patrikalakis and H. Gürsoy. *Shape Interrogation by Medial Axis Transform.* Technical Report Memo 90-2, MIT, Ocean Engr. Design Lab, 1990.

[22] F. Preparata. The medial axis of a simple polygon. In *Proc. 6th Symp. Mathematical Foundations of Comp. Sci.*, pages 443–450, 1977.

[23] M. Price, T. Tam, C. Armstrong, and R. McKeag. Computing the branch points of the voronoi diagram of a object using a point Delaunay triangulation algorithm. 1991. Draft manuscript.

[24] A. Requicha. *Mathematical Models of Rigid Solids.* Technical Report Memo 28, University of Rochester, Production Automation Project, 1977.

[25] A. Rosenfeld and J. Pfaltz. Sequential operations in digital picture processing. *Journal of the ACM*, 13:471–494, 1966.

[26] H. J. Samet. *Design and analysis of Spatial Data Structures: Quadtrees, Octrees, and other Hierarchical Methods.* Addison–Wesley, Redding, MA, 1989.

[27] N. Sapidis and R. Perucchio. Domain Delaunay tetrahedrization of arbitrarily shaped curved polyhedra defined in a solid modeling system. In *Proc. ACM/SIGGRAPH Symp Solid Modeling Found and CAD/CAM Applic*, Austin, Tex, 1991.

[28] V. Srinivasan and L. Nackman. Voronoi diagram of multiply connected polygonal domains. *IBM Journal of Research and Development*, 31:373–381, 1987.

[29] V. Srinivasan, L. Nackman, J. Tang, and S. Meshkat. *Automatic Mesh Generation using the Symmetric Axis Transformation of Polygonal Domains.* Technical Report RC 16132, IBM Yorktown Heights, 1990.

[30] S. Stifter. An axiomatic approach to Voronoi diagrams in 3d. *Journal of Computer and System Sciences*, to appear, 1991.

[31] G. Strang. *Introduction to Applied Mathematics.* Wellesley-Cambridge Press, Wellesley, MA, 1986.

[32] K. Strubecker. *Differentialgeometrie III.* Sammlung Göschen Bd. 1180/1180a, Walter de Gruyter, Berlin, Germany, 1969.

[33] A. Wallis, D. Lavender, A. Bowyer, and J. Davenport. Computing voronoi diagrams of geometric models. In *IMPA Workshop on Geometric Modeling*, Rio de Janeiro, 1991.

[34] X. Yu, J. A. Goldak, and L. Dong. Constructing 3D discrete medial axis. In *Proc. ACM Symp. Solid Modeling Found. and CAD/CAM Applic.*, pages 481–492, Austin, 1991.